Cellular/Molecular

Neurofibromin Mediates FAK Signaling in Confining Synapse Growth at *Drosophila* Neuromuscular Junctions

Pei-I Tsai,[1,2] Manyu Wang,[1,2] Hsiu-Hua Kao,[1] Ying-Ju Cheng,[1] James A. Walker,[3] Ruey-Hwa Chen,[2,4] and Cheng-Ting Chien[1,2]

[1]Institute of Molecular Biology, Academia Sinica, Taipei 115, Taiwan, [2]Institute of Molecular Medicine, National Taiwan University, Taipei 106, Taiwan, [3]Massachusetts General Hospital Center for Cancer Research and Harvard Medical School, Charlestown, Massachusetts 02129, and [4]Institute of Biological Chemistry, Academia Sinica, Taipei 115, Taiwan

Neurofibromatosis type I (NF1), caused by the mutation in the *NF1* gene, is characterized by multiple pathological symptoms. Importantly, ~50% of NF1 patients also suffer learning difficulty. Although downstream pathways are well studied, regulation of the *NF1*-encoded neurofibromin protein is less clear. Here, we focused on the pathophysiology of *Drosophila NF1* mutants in synaptic growth at neuromuscular junctions. Our analysis suggests that the *Drosophila* neurofibromin protein NF1 is required to constrain synaptic growth and transmission. NF1 functions downstream of the *Drosophila* focal adhesion kinase (FAK) Fak56 and physically interacts with Fak56. The N-terminal region of NF1 mediates the interaction with Fak56 and is required for the signaling activity and presynaptic localization of NF1. In presynapses, NF1 acts via the cAMP pathway, but independent of its GAP activity, to restrain synaptic growth. Thus, presynaptic FAK signaling may be disrupted, causing abnormal synaptic growth and transmission in the NF1 genetic disorder.

Introduction

The hereditary disorder neurofibromatosis type I (NF1), caused by mutations in the *NF1* gene, is characterized by multiple pathological symptoms, such as multiple cafe-au-lait spots and neurofibromas. Approximately 50% of NF1 patients also suffer learning disability (Allanson et al., 1991; von Deimling et al., 1995; Friedman, 1999; Costa et al., 2001; Arun and Gutmann, 2004). *NF1* mutations cause reduction in the level and/or activity in the protein neurofibromin that carries a Ras GAP-related domain (GRD) (Wallace et al., 1990). In several cases, abnormality in *NF1* animal models can be attributed to disregulated Ras/MAPK signaling (Gutmann et al., 1993; Weiss et al., 1999; Tong et al., 2002). In *Drosophila, NF1* mutants display growth retardation primarily caused by hyperactivated Ras signaling, which can be rescued by neuronal expression of the *NF1* gene (The et al., 1997; Walker et al., 2006). Circadian rhythm in *NF1* mutants is also disturbed by hyperactivated Ras/MAPK signaling (Williams et al., 2001). The second pathway known to mediate neurofibromin/NF1 activity is adenylyl cyclase (AC)/cAMP signaling. Reduced AC activity contributes to the phenotypes observed in $NF1^{-/-}$ mouse brain (Tong et al., 2002). Several defects in *NF1* mutant flies are caused by disregulated AC/cAMP signaling, such as shortened life span, diminished neuropeptide-stimulated K^+ current, and defective olfactory learning and memory (Guo et al., 1997, 2000; Tong et al., 2007). Thus, Ras/MAPK and AC/cAMP mediate different cellular functions of neurofibromin/NF1 in animals. Molecularly, the GRD of neurofibromin/NF1 catalyzes turnover of Ras-GTP while the C-terminal domain is involved in AC activation (Weiss et al., 1999; Tong et al., 2002). Although downstream signaling pathways are well studied, regulation of neurofibromin/NF1 activities and upstream signaling components are not clear.

Focal adhesion kinase (FAK) functions in cerebral cortex lamination, growth cone dynamics, axon branching and pathfinding, and synapse formation (Beggs et al., 2003; Rico et al., 2004; Robles and Gomez, 2006; Endo and Yamashita, 2009; Woo et al., 2009; Myers and Gomez, 2011). FAK functions together with Src in netrin and integrin signaling to modulate axonal terminal dynamics (Li et al., 2004; Liu et al., 2004; Ren et al., 2004; Robles and Gomez, 2006). FAK also suppresses axonal arborization through a p190RhoGEF-dependent mechanism (Rico et al., 2004). In EphB-receptor signaling, FAK inhibits the activity of the F-actin-severing protein cofilin to maintain dendritic spine stability in hippocampal neurons (Shi et al., 2009). The *Drosophila* FAK, Fak56, confines synaptic growth and regulates basal synaptic transmission at neuromuscular junctions (NMJs) (Tsai et al., 2008).

We examined morphological and electrophysiological properties at NMJs of *Drosophila NF1* mutants, and found that they displayed the same phenotypes as *Fak56* mutants. Genetic and

Received April 11, 2012; revised Aug. 20, 2012; accepted Sept. 17, 2012.

Author contributions: P.-I.T., R.-H.C., and C.-T.C. designed research; P.-I.T., M.W., H.-H.K., and Y.-J.C. performed research; J.A.W. contributed unpublished reagents/analytic tools; P.-I.T., M.W., and H.-H.K. analyzed data; P.-I.T., R.-H.C., and C.-T.C. wrote the paper.

This work was supported by grants from Academia Sinica and the National Science Council to C.-T.C. We thank N.H. Brown, R. Palmer, Y. Zhong, the Developmental Studies Hybridoma Bank, the Drosophila Genomics Resource Center, the Bloomington Drosophila Stock Center, and the Vienna Drosophila RNAi Center for fly stocks and antibodies. We are grateful to S.-P. Lee and S.-P. Tsai at the Institute of Molecular Biology Image Facility for assistance with confocal and electron microscopy. We also thank laboratory members in the laboratories of Drs. Chien and Chen for suggestions.

The authors declare no competing financial interests.

Correspondence should be addressed to Cheng-Ting Chien, Institute of Molecular Biology, Academia Sinica, 128 Academia Road, Section 2, Nankang, Taipei 115, Taiwan. E-mail: ctchien@gate.sinica.edu.tw.

DOI:10.1523/JNEUROSCI.1756-12.2012

 0270-6474/12/3216971-11$15.00/0

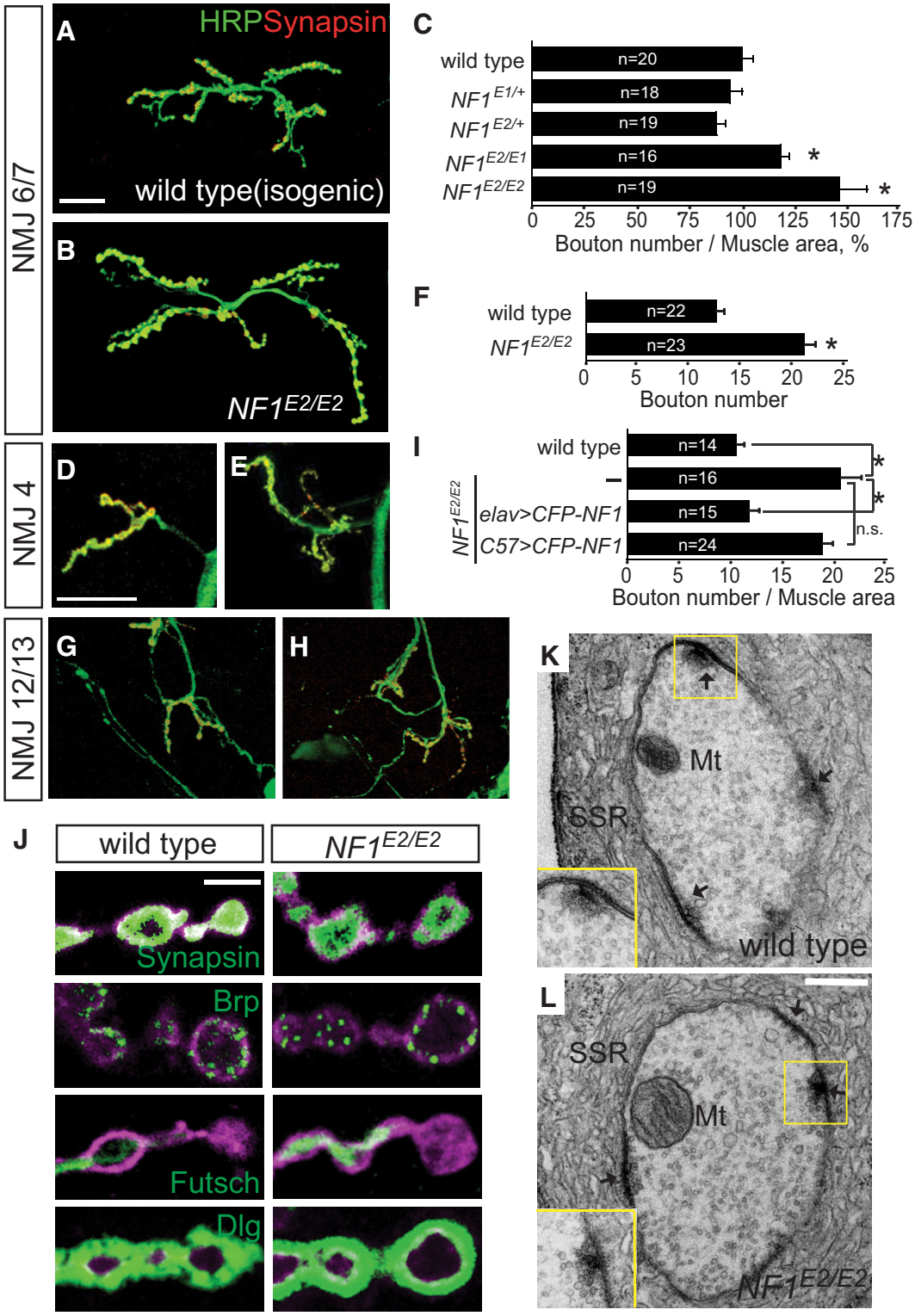

Figure 1. Presynaptic function of NF1 in NMJ growth regulation. ***A***, ***B***, ***D***, ***E***, ***G***, ***H***, NMJ 6/7s (***A***, ***B***), NMJ 4s (***D***, ***E***), and NMJ 12/13s (***G***, ***H***) are shown by labeling for HRP (green) and Syn (red) in wild type (***A***, ***D***, ***G***) and $NF1^{E2/E2}$ (***B***, ***E***, ***H***). Scale bars: ***A***, ***D***, ***G***, 20 μm. ***C***, ***F***, NMJ sizes quantified as bouton numbers divided by muscle areas for NMJ 6/7s, shown as bouton number times 10^{-4}/muscle area (μm^2), which were then normalized to wild-type control 100% (***C***) or bouton numbers for NMJ 4s (***F***). Average NMJ sizes (mean ± SEM) in this and all following figures were compared by Student's *t* test for statistical significance, with asterisk indicating $p < 0.05$, and no significance (n.s.) for $p > 0.05$. Sample number (*n*) is shown within bar. ***I***, NMJ overgrowth in $NF1^{E2}$ was rescued by presynaptic expression of *UAS-CFP-NF1* (*elav>CFP-NF1* $NF1^{E2/E2}$) but not postsynaptic expression (*C57>CFP-NF1* $NF1^{E2/E2}$). ***J***, Expressions of Syn in presynapses, Brp at active zones, Futsch for microtubules, and Dlg in postsynapses are shown for wild-type control (left) and $NF1^{E2/E2}$ (right) at NMJ 4s that were costained with HRP (magenta). All images are shown as single sections. Scale bar, 5 μm. ***K***, ***L***, Electron micrographs of cross sections through a type I bouton of muscle 6/7s of wild type (***K***) and $NF1^{E2/E2}$ (***L***) larvae reared at 22°C. Squares show active zones with a T-bar, which are enlarged in lower left corner. Subsynaptic reticula (SSR), active zones (arrows), and mitochondria (Mt) are indicated. Scale bar, 0.2 μm.

protein–protein interaction between NF1 and Fak56 suggested that NF1 functions downstream of and forms a protein complex with Fak56 through the N-terminal 400 aa region that mediates NF1 signaling activity and synaptic localization. We further showed that the GAP activity of NF1 is dispensable while the AC/cAMP pathway is required to mediate NF1 and Fak56 in presynapses to suppress NMJ growth.

Materials and Methods

Fly stocks and manipulations. Drosophila larvae of both sexes were used in this study. Wild-type control is w^{1118} or an isogenic strain for *NF1* mutants. Mutant alleles were backcrossed to w^{1118} for at least five generations. $Fak56^{N30}$, $Fak56^{K24}$, $Fak56^{KG00304}$, rut^{1}, dnc^{M14}, $NF1^{E1}$, $NF1^{E2}$, $NF1^{P2}$, *hs-NF1 wt, hs-NF1 K1481A, hs-NF1 R1276P*, and *hs-NF1* Δ*GRD* have been previously reported (Zhong et al., 1992; The et al., 1997; Devenport and Brown, 2004; Walker et al., 2006; Tsai et al., 2008). *UAS-NF1-A*, *UAS-NF1-B*, *UAS-CFP-NF1*, and *UAS-CFP-NF1*Δ*A* were constructed for this study using the Gateway System (Invitrogen and *Drosophila* Genomics Resource Center). GAL4 drivers *elav-GAL4* and *C57-GAL4* were obtained from the Bloomington Drosophila Stock Center. *UAS-rut RNAi (II* and *III)* were from the Vienna Drosophila RNAi Center. All flies were reared at 25°C.

Immunostaining of NMJs and imaging processing. Larvae of wandering late third instar were dissected for analyzing NMJ phenotypes at A3 segments, as previously described (Tsai et al., 2008). Primary antibodies used were for synapsin (Syn) [3C11, 1:100; Developmental Studies Hybridoma Bank (DSHB)], Bruchpilot (Brp) (nc82, 1:100; DSHB), Futsch (22C10, 1:100; DSHB), Discs large (Dlg) (4F3, 1:100; DSHB), Fas2 (1D4, 1:100; DSHB), FAK [pY^{397}] (rabbit, 1:50; Invitrogen), GFP (mouse, 1:500; Invitrogen), HRP-conjugated TRITC or Cy5 (rabbit, 1:100; Jackson ImmunoResearch). Images were acquired using confocal Zeiss LSM 510 Meta and processed by Adobe Photoshop CS. Quantification of NMJ bouton numbers were collected by projecting images from 10 *z*-sections within 6.5–8 μm. The NMJ 6/7 size was shown as bouton numbers divided by muscle areas revealed by phalloidin staining and measured by Zeiss LSM Image Examiner.

Electronic microscopy of boutons. The procedure has been described (Tsai et al., 2008). Briefly, dissected larval body walls with attached ventral nerve cords and motor axons were fixed in modified Trump's fixative and postfixed in 2% osmium tetroxide in 0.1 M sodium cacodylate buffer. The dissected muscle 6/7s of A3 segments were stained en bloc in 2% aqueous uranyl acetate, dehydrated in a graded ethanol series, and embedded in the Spurr's medium. Thin sections (90 nm) were stained with uranyl acetate and lead citrate, and imaged from a Tecnai G2 Spirit TWIN electron microscope (FEI) and a Gatan CCD Camera (794.10.BP2 MultiScan). TEM data were quantified by MetaMorph V6.3r7 (Molecular Devices).

Preparation of dibutyryl-cAMP-supplemented or forskolin-supplemented larval food. The stock solutions of dibutyryl-cAMP (db-cAMP) and forskolin (Sigma-Aldrich) were prepared in distilled water and DMSO, respectively. The stock solutions or solvents (mock controls) were added into food vials to reach final concentrations of 10 μM, which was repeated every 2 d while larvae were growing to reach late third instar.

Immunoprecipitation, immunoblotting, and GST pull-down assay. Embryos of 0–24 h or transfected S2 cells were homogenized in lysis buffer (100 mM NaCl, 10 mM Tris, pH 7.6, 1 mM EDTA, 1% Triton X-100, 10 mM glycerol phosphate, 10 mM NaF, 1 mM Na_3VO_4, 1 mM PMSF, 10 μg/ml aprotinin, and 10 μg/ml leupeptin). Lysates of 1.5 mg of total protein were used for immunoprecipitation by anti-NF1 (guinea pig; Walker et al., 2006) or anti-Flag (1:20,000 dilution; M2; Sigma-Aldrich) antibodies. For Western blots, anti-Fak56 (rabbit, 1:5000; Palmer et al., 1999), anti-NF1 (Mab11, 1:1; Walker et al., 2006), anti-phosphotyrosine (1:1000; 4G10; Millipore) and anti-Myc (1:3000; 9E10; Santa Cruz Biotechnology) antibodies were used. Seven NF1 cDNA fragments (see Fig. 4*A* for the range of each fragment) were subcloned into pGEX4T-3. GST-NF1 fusion proteins were expressed, purified, and immobilized on glutathione beads and incubated with 500 μg of total protein from S2 cell lysates made in radioimmunoprecipitation assay lysis buffer (150 mM NaCl, 50 mM Tris, pH 7.5, 1% sodium deoxycholate, 1% NP40, 0.1% SDS, 1 mM PMSF, 10 μg/ml aprotinin, and 10 μg/ml leupeptin). The GST pull-down complexes were analyzed by Western blot using anti-Fak56 antibodies.

Electrophysiological recording. The basal transmission properties were measured in muscle 6 of A3 segments as previously described (Tsai et al., 2008). Briefly, larval body walls were dissected in cold (4°C) HL3.1 Ca^{2+}-free saline (Feng et al., 2004) and recorded in HL3.1 containing 0.2–0.4 mM $CaCl_2$ at 22°C. Only samples with resting potential from −80 to −65 mV and membrane resistance of >5 MΩ were measured. The measured excitatory junction potential (EJP) amplitudes were corrected for nonlinear summation by using two different correction factors (Stevens, 1976; McLachlan and Martin, 1981). Paired-pulse facilitation (PPF) is the ratios of second EJPs to first EJPs, averaged from responses to 3–5 consecutive stimulations (separated by 10 s rest) at 20–500 ms interpulse intervals. Signals were digitized at 50 kHz by a DigiData 1440 interface (Molecular Devices), low-pass filtered at 10 kHz, and saved on IBM-compatible PC for analysis.

Table 1. Features of synaptic ultrastructures were quantified, and statistical significances (*p* value) between wild type and $NF1^{E2/E2}$ calculated by Student's *t* test are shown in right column

	wild type ($n = 16$)	$NF^{E2/E2}$ ($n = 15$)	*p* Value
Single bouton area (μm^2)	5.07 ± 1.06	4.98 ± 0.69	0.947
Bouton perimeter (μm)	7.83 ± 0.65	8.24 ± 0.57	0.640
Active zone #/bouton	5.00 ± 0.44	4.13 ± 0.45	0.176
Active zone length/bouton (μm)	2.68 ± 0.25	2.69 ± 0.32	0.972
Active zone length/bouton perimeter	0.34 ± 0.02	0.31 ± 0.02	0.286
T-bar number/bouton	2.06 ± 0.25	1.93 ± 0.23	0.705
Bouton area (μm^2)/active zone	0.96 ± 0.12	1.22 ± 0.13	0.141
T-bar number/active zone	0.41 ± 0.04	0.48 ± 0.04	0.165

Results

Presynaptic NF1 suppresses NMJ growth

To examine whether NF1 has a role in NMJ growth regulation, we examined NMJ morphology of late third instar homozygous or transheterozygous for $NF1^{E1}$ and $NF1^{E2}$, compared with isogenic wild-type control. NMJ morphology is revealed by immunostaining for HRP labeling axonal processes and Syn labeling presynaptic vesicles (Fig. 1*A*). Also, muscle fibers were labeled by phalloidin (data not shown). Both $NF1^{E1/+}$ and $NF1^{E2/+}$ heterozygotes show no difference to wild-type control, which is an isogenic line used to generate these two alleles. However, both $NF1^{E2/E2}$ and $NF1^{E1/E2}$ displayed larger NMJ size (Fig. 1*B*,*C*), suggesting that $NF1^{E2}$ is a stronger allele than $NF1^{E1}$ in NMJ growth control. The overgrowth phenotype is not limited to NMJ 6/7s as the sizes of NMJ 4s and NMJ 12/13s were also increased in $NF1^{E2/E2}$ (Fig. 1*D–H*). *NF1* mutants also display smaller body and muscle size (Walker et al., 2006). However, the increase in NMJ size was not attributed to the reduction in muscle size, as muscle expression of *UAS-CFP-NF1* by the *C57-GAL4* driver restored the muscle size but failed to suppress the overgrowth of NMJs in $NF1^{E2/E2}$ (Fig. 1*I*). In contrast, neuronal expression of *UAS-CFP-NF1* suppressed NMJ overgrowth, indicating that NF1 is required in presynapses in NMJ growth control (Fig. 1*I*).

The overgrown NMJs in $NF1^{E2/E2}$ showed normal distribution of synaptic proteins analyzed by immunostaining. These proteins include synaptic vesicle-localized Syn, active zone-localized Brp, microtubule-associated Futsch, and postsynaptic PDZ-protein Dlg (Fig. 1*J*). In addition, analysis by transmission electron microscopy revealed normal morphology and size of boutons and subsynaptic reticula, and distribution of ultrastructures, such as active zones and T-bars (Fig. 1*K*,*L*, Table 1). These results suggest

that NF1 functions in presynapses to confine normal NMJ growth during larval development.

Synaptic transmission is increased in *NF1* mutants

To examine whether NF1 contributes to the transmitter release, postsynaptic responses were recorded at *NF1* mutant NMJs (Fig. 2*A*,*B*). When compared with the isogenic wild-type control, the amplitude of evoked junctional potential (EJP) was increased by 67% in $NF1^{E2/E2}$ (wild type: 12.04 ± 1.75 mV; $NF1^{E2/E2}$: 20.13 ± 1.66 mV; $p = 0.003$, Student's *t* test). To determine whether the increase in the EJP amplitude in $NF1^{E2/E2}$ was caused by greater response from postsynaptic glutamate receptors or by increased release probability of presynaptic vesicles, we compared spontaneous release [or miniature EJP (mEJP)] between wild type and *NF1* mutants. Whereas the amplitude of mEJP remained constant in $NF1^{E2/E2}$ (wild type: 1.04 ± 0.11 mV; $NF1^{E2/E2}$: 0.97 ± 0.06 mV; $p = 0.592$, Student's *t* test), a slight increase, although not statistically significant, was detected in the frequency of mEJP (wild type: 1.65 ± 0.19 Hz; $NF1^{E2/E2}$: 2.08 ± 0.17 Hz; $p = 0.104$, Student's *t* test). The similarity in mEJP amplitudes suggests that the postsynaptic response was largely normal in $NF1^{E2/E2}$ mutants. Instead, the quantal content, calculated by dividing EJP with mEJP, was significantly increased in $NF1^{E2/E2}$ mutants (wild type: 12.61 ± 2.39; $NF1^{E2/E2}$: 21.52 ± 2.02; $p = 0.009$, Student's *t* test). These changes in basal transmission properties suggest that NF1 likely regulates presynaptic release probability.

To further study the increase in the release probability, we measured EJPs in different Ca^{2+} concentrations. The EJP difference between wild type and $NF1^{E2/E2}$ was largest at 0.2 mM, decreased at 0.3 mM, and diminished at 0.4 mM (Fig. 2*C*). Thus, $NF1^{E2/E2}$ mutant EJP amplitudes are higher when the Ca^{2+} concentration is low. We chose 0.3 mM Ca^{2+} for performing PPF. At wild-type NMJ 6/7s, the second pulse was consistently larger than the first pulse at all interstimulus intervals. In $NF1^{E2/E2}$ mutants, while the PPF was still detected, the second pulse was significantly reduced at all interstimulus intervals (Fig. 2*D*), consistent with the idea that the release probability at $NF1^{E2/E2}$ NMJs is increased.

The increase in the EJP amplitude was also detected in $NF1^{E1/E2}$ (Fig. 2*E*). To address whether NF1 functions in presynapses or postsynapses to regulate the evoked release, we performed rescue experiments in $NF1^{E2/E2}$. When *UAS-CFP-NF1* was driven by *elav-GAL4*, the EJP amplitude was restored to almost wild-type levels (102 ± 10% of wild type, $p = 0.016$). While postsynaptic expression also suppressed the enlarged EJP amplitude, it was not statistically significant (116 ± 8% of wild type, $p = 0.074$). Thus, NF1 mainly functions in presynapses to regulate synaptic transmission.

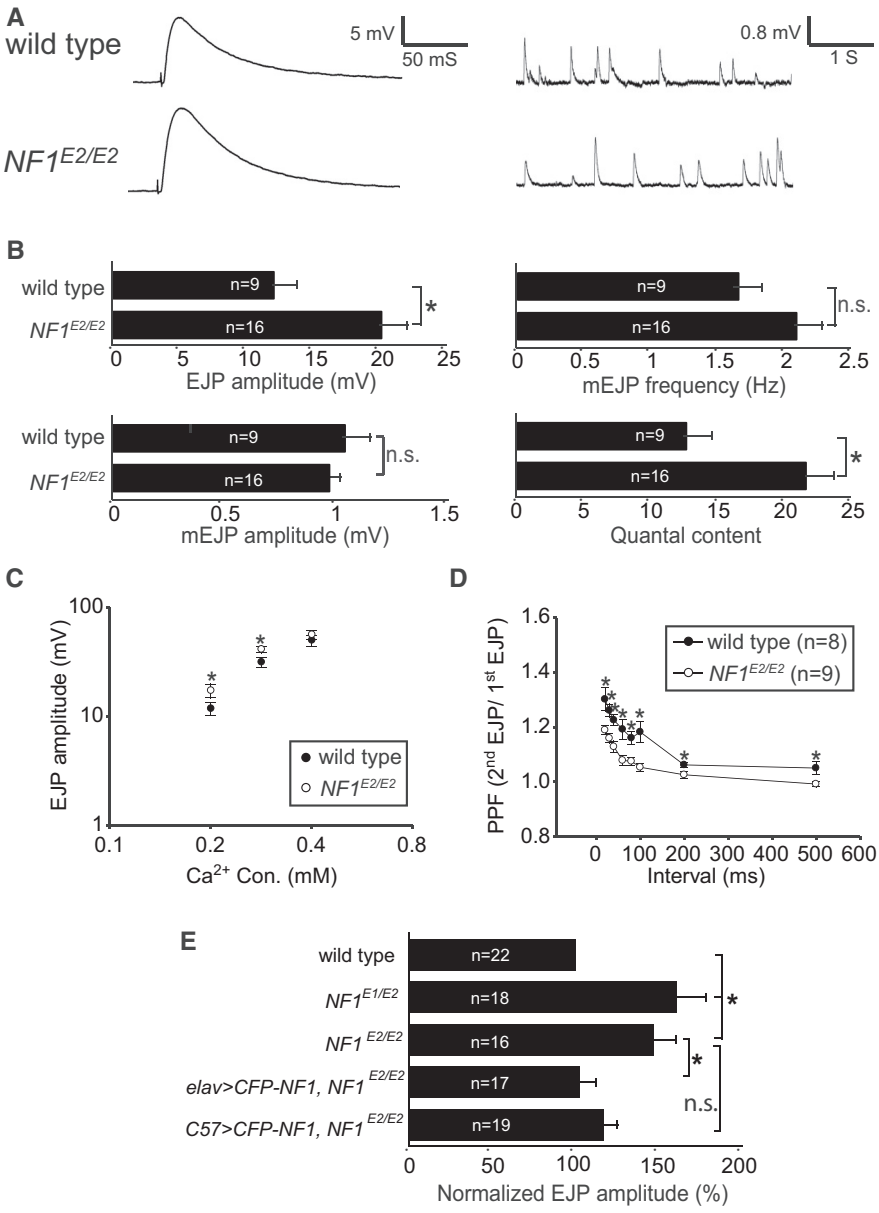

Figure 2. Synaptic transmission properties in $NF1^{E2/E2}$. ***A***, Electrophysiological recordings at muscle 6s of wild type and $NF1^{E2/E2}$, showing a representative EJP or mEJP trace for each. Resting potentials: wild type, −75.69 ± 2.10 mV; $NF1^{E2/E2}$, −73.23 ± 1.60 mV. ***B***, Average EJP amplitude, mEJP amplitude, mEJP frequency, and quantal content in wild type and $NF1^{E2/E2}$ are shown. ***C***, EJP amplitudes in 0.2, 0.3, and 0.4 mM Ca^{2+} concentrations in wild type (close symbols) and $NF1^{E2/E2}$ (open symbols) with at least 10 samples in each average EJP. ***D***, Measurement of PPFs for wild type and $NF1^{E2/E2}$ with interstimulus intervals between 20 and 500 ms. ***E***, Comparison of EJPs in $NF1^{E1/E2}$ and $NF1^{E2/E2}$ mutants and rescue of EJPs in $NF1^{E2/E2}$ by *elav-GAL4* or *C57-GAL4* drivers. The EJP is shown as percentages to wild type (100%). In all comparisons in this figure, significant difference is indicated by asterisk with $p < 0.05$ by Student's *t* test. Not significant (n.s.), $p > 0.05$. The *p* values are 0.016 between $NF1^{E2}$ and *elav>CFP-NF1* $NF1^{E2/E2}$ and 0.074 between $NF1^{E2}$ and *elav>CFP-NF1* $NF1^{E2/E2}$. Resting potentials: wild type, −73.10 ± 1.37 mV; $NF1^{E1/E2}$, −72.29 ± 1.36 mV; $NF1^{E2/E2}$, −73.23 ± 1.60 mV; *elav>CFP-NF1* $NF1^{E2}$, −69.42 ± 1.26 mV; *C57>CFP-NF1* $NF1^{E2}$, −69.94 ± 1.40 mV.

NF1 physically interacts with Fak56

Similar to *NF1*, *Fak56* functions in presynapses to regulate NMJ growth and synaptic transmission properties (Tsai et al., 2008). We then tested the genetic interaction between *Fak56* and *NF1*.

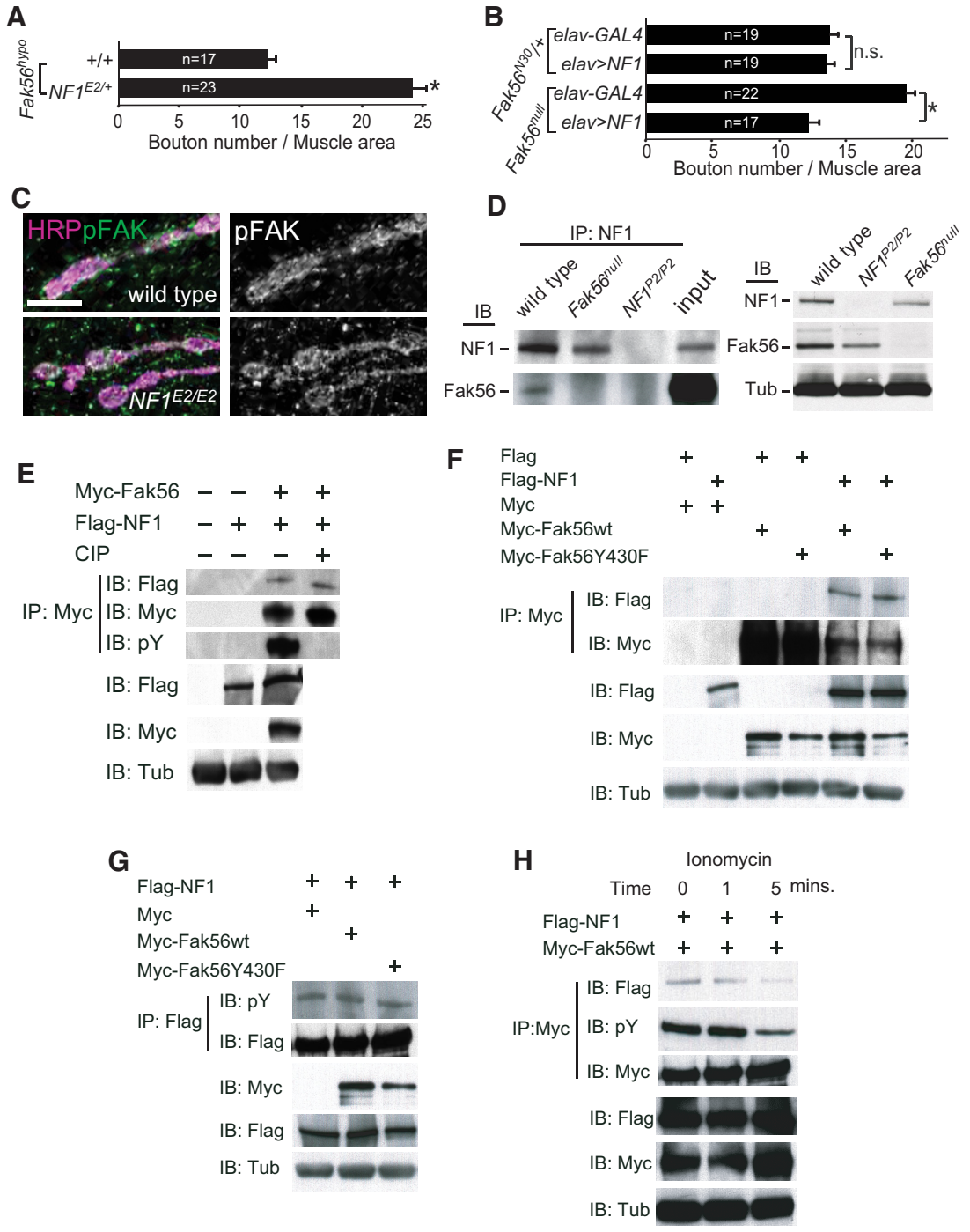

Figure 3. Genetic and protein–protein interaction between Fak56 and NF1. ***A***, ***B***, Quantification of NMJ 6/7 size was done as for Figure 1*C*. ***A***, Enhancement of *Fak56*^{hypo} NMJ 6/7 growth by *NF1*^{E2} in *Fak56*^{hypo};*NF1*$^{E2/+}$. ***B***, Rescue of *Fak56*^{null} NMJ overgrowth by *elav-GAL4* expression of *NF1* by comparing NMJ 6/7 sizes between *elav-GAL4;Fak56*^{null} and *elav*>*CFP-NF1;Fak56*^{null}, and *elav-GAL4;Fak56*$^{N30/+}$ and *elav*>*NF1-CFP;Fak56*$^{N30/+}$ as controls. ***C***, pFAK signals shown in green (left) or white (right) are indistinguishable between wild-type and *NF1*$^{E2/E2}$ NMJs costained with HRP in magenta. Scale bar, 5 μm. ***D***, Coimmunoprecipitation of Fak56 and NF1. NF1 immunoprecipitates from embryo extracts were blotted by NF1 and Fak56 antibodies (left). Input control, 2% of wild-type extracts. As control for antibody specificity, wild type, *NF1*$^{P2/P2}$, and *Fak56*^{null} were blotted by Fak56, NF1, or tubulin (Tub) antibodies (right). ***E–G***, Phosphorylation-independent complex formation between Fak56 and NF1. ***E***, S2 cells transfected with Myc-Fak56 and Flag-NF1 were immunoprecipitated by Myc antibody and treated with or without the alkaline calf intestine phosphatase (CIP). Top, Detection of NF1 levels showed no difference between wild type and *NF1*$^{E2/E2}$ mutant. ***F***, ***G***, S2 cells transfected with Myc, Myc-Fak56, or Myc-Fak56Y430F with Flag-NF1 (***F***, ***G***) or Flag (***F***) were immunoprecipitated by Myc antibodies, and immunoblotted by Myc or Flag antibodies to reveal NF1 and Fak56 levels (***F***, top), or immunoprecipitated by Flag antibody, and immunoblotted with pY or Flag antibodies (***G***, top two panels). As control, S2 cell extracts were blotted by Flag, Myc, or Tub antibodies without immunoprecipitation. ***H***, S2 cells transfected with Flag-NF1 and Myc-Fak56 and treated with 6 mM ionomycin for 0, 1, and 5 min. The Myc immunoprecipitates were blotted with Flag, pY, and Myc antibodies (top). Total cell extracts without immunoprecipitation were also blotted with Flag, Myc, and Tub antibodies (bottom).

The normal NMJ size in hypomorphic *Fak56*$^{N30/KG}$ (*Fak56*^{hypo}) was enhanced by the *NF1*^{E2} allele (Fig. 3*A*). The strong genetic interaction prompted us to test whether *Fak56* and *NF1* function in the same pathway in NMJ growth regulation. Importantly, while presynaptic expression of *NF1-CFP* had no effect on the normal NMJ growth in the heterozygous *Fak56*$^{N30/+}$ mutant, it fully suppressed the overgrown NMJ in the *Fak56*-null mutant (*Fak56*$^{N30/K24}$, Fig. 3*B*), suggesting that NF1 functions down-

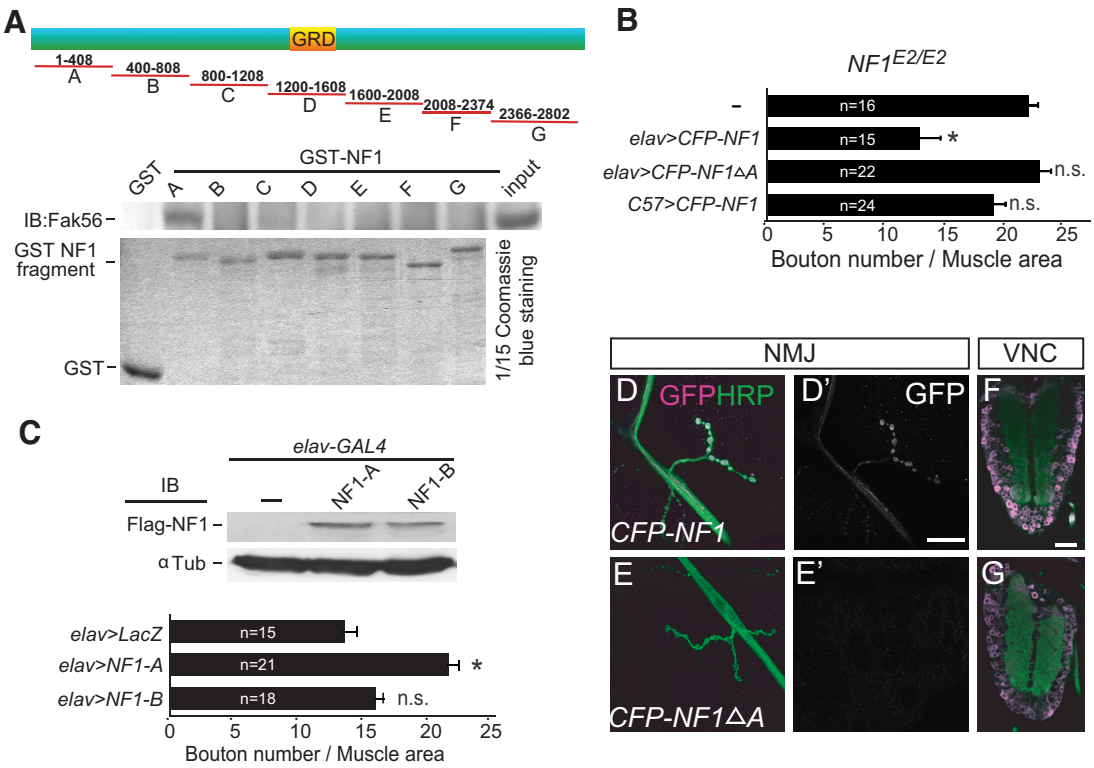

Figure 4. The N-terminal A region mediates Fak56 interaction and NF1 synaptic localization. ***A***, The A region of NF1 precipitates with Fak56. NF1 was divided into seven fragments to generate GST fusions (GST-NF1A to NF1G, top diagram). The GRD and the size of each fragment are indicated. GST-NF1 fusions were purified (bottom) for pull-down assays in S2 cell extracts, and the precipitates were blotted with Fak56 antibodies (middle). ***B***, The A region is required for NF1 activity in regulating NMJ size in $NF1^{E2/E2}$. Quantification of NMJ 6/7 size, as done in Figure 1*C*, showing neuronal expression of NF1 ($NF1^{E2/E2}$; *elav>CFP-NF1*) or A region-truncated NF1 ($NF1^{E2/E2}$; *elav>CFP-NF1ΔA*), or muscle expression of NF1 ($NF1^{E2/E2}$; *C57>CFP-NF1*). ***C***, Dominant-negative effect of the A region in causing NMJ overgrowth. Quantification of NMJ 6/7 size in *elav>LacZ*, *elav>NF1-A*, and *elav>NF1-B* (bottom). Expression levels of Flag-NF1-A and Flag-NF1-B by *elav-GAL4* in adult brain are shown in Flag Western blot (top). The *elav>LacZ* serves as control. *$p < 0.05$ by Student's *t* test. ***D–G***, NF1 expressions detected by the GFP antibody (***D′***, ***E′***, magenta or white) at axons and NMJs of *elav>CFP-NF1* (***D***) but not *elav>CFP-NF1ΔA* (***E***) costained with HRP (green). Both were detected in ventral nerve cords (***F***, ***G***). Scale bars: ***D′***, 20 μm; ***F***, 50 μm.

stream of or in parallel to Fak56 in NMJ growth regulation. As presynaptic overexpression of *Fak56* by several neuronal GAL4 drivers caused embryonic lethality, we were unable to perform the reverse experiment of rescuing $NF1^{E2/E2}$ NMJ overgrowth by *Fak56*. In line with the notion that Fak56 acts upstream of or in parallel to NF1, the level of Fak56 tyrosine phosphorylation, an indication for the activation of integrin signaling, remained normal at $NF1^{E2}$ NMJs (Fig. 3*C*). Together, these results are most consistent with the notion that NF1 functions downstream of Fak56 in regulating NMJ growth.

We next examined whether NF1 physically interacts with Fak56. In NF1 immunoprecipitates from embryonic extracts, Fak56 was detected by anti-FAK antibodies in Western blot analysis. As controls, NF1-immunoprecipitates from *Fak56* or *NF1* mutant extracts failed to reveal any Fak56 signal (Fig. 3*D*, right). In addition, Flag-tagged NF1 and Myc-tagged Fak56 proteins in S2 cells also existed in the same immunocomplex (Fig. 3*E–H*). Thus, NF1 and Fak56 either interact with each other directly or exist within the same protein complex.

Tyrosine phosphorylation of FAK mediates FAK interaction with diverse proteins for signaling activities (Mitra et al., 2005). However, the Flag-NF1/Myc-Fak56 complex was not dissociated upon the treatment with calf intestine phosphatases (Fig. 3*E*, lane 4). Furthermore, Myc-Fak56Y430F with mutation in the autophosphorylation site associated with Flag-NF1 as efficiently as Myc-Fak56wt (Fig. 3*F*). Furthermore, overexpression of Myc-Fak56wt or Myc-Fak56Y430F failed to alter the level of tyrosine phosphorylation on NF1 (Fig. 3*G*). These results suggest that the Fak56-NF1 interaction is independent of Fak56 tyrosine phosphorylation activity.

We next tested whether Ca^{2+} influx regulates the interaction between Fak56 and NF1. Elevation of the Ca^{2+} influx by treatment of S2 cells with ionomycin diminished the interaction between NF1 and Fak56 (Fig. 3*H*), suggesting that the interaction between NF1 and Fak56 is Ca^{2+}-sensitive. Consistent with a previous report (Ueda et al., 2008), the level of tyrosine-phosphorylated Fak56 was also reduced in response to ionomycin (Fig. 3*H*). Because the interaction between NF1 and Fak56 was independent of tyrosine phosphorylation, intracellular Ca^{2+} concentration likely affects the Fak56-NF1 association and Fak56 tyrosine phosphorylation independently.

The N-terminal A region of NF1 is required for Fak56 interaction and presynaptic localization

The Fak56–NF1 interaction may function to recruit or stabilize NF1 to the presynaptic sites. To test this, we first defined the interacting region of NF1 by the GST pull-down assay. Seven GST fusion proteins (NF1-A–NF1-G) with overlapping *NF1* sequence were generated to test interaction with Fak56. Only NF1-A (amino acids 1–408) was able to pull down Fak56 (Fig. 4*A*). Further deletion analysis within the NF1-A region failed to reveal smaller Fak56-interacting regions, suggesting that the intact A region or >1 motifs within NF1-A are required for Fak56 interaction.

We further tested whether the A region is required for NF1 to regulate NMJ growth. While the full-length NF1 (*CFP-NF1*)

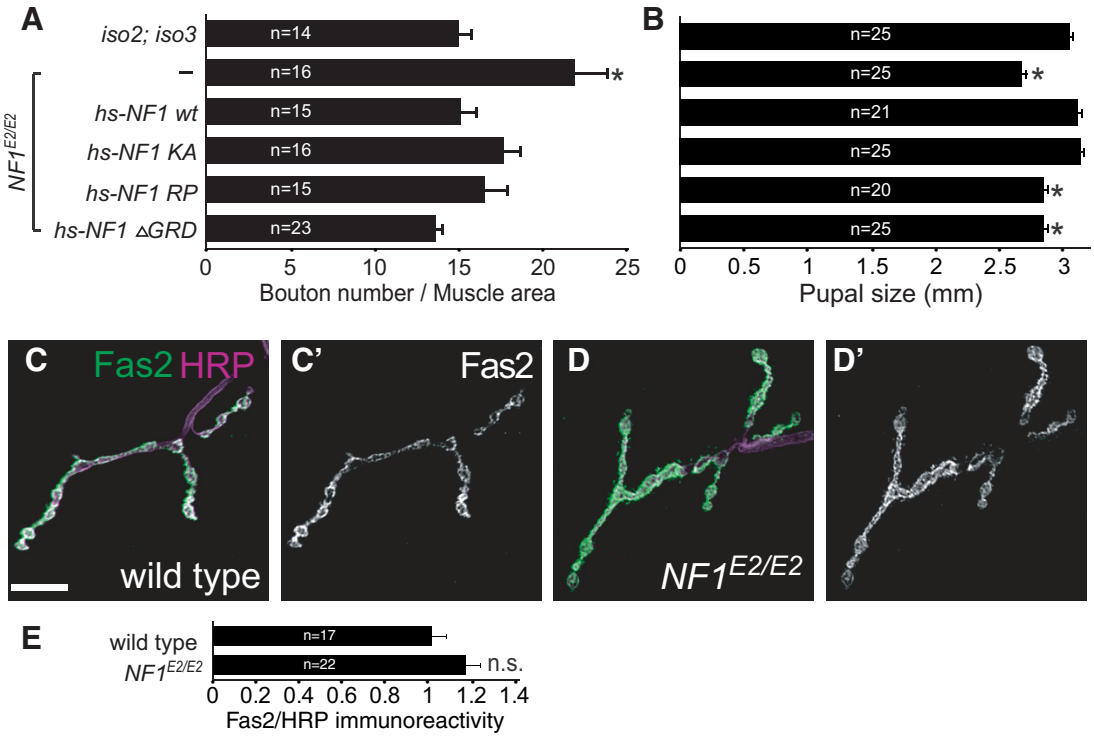

Figure 5. Suppression of NMJ growth by NF1 is independent of RasGAP activity. ***A***, ***B***, Quantification of the NMJ 6/7 size (***A***), as done in Figure 1*C*, and the length of pupal cases (***B***), measured at 48 h after puparium formation, are compared between wild type, and $NF1^{E2/E2}$, $NF1^{E2/E2}$ *hs-NF1 wt*, $NF1^{E2/E2}$ *hs-NF1 KA*, $NF1^{E2/E2}$ *hs-NF1 RP*, and $NF1^{E2/E2}$ *hs-NF1* Δ*GRD*. All transgenics were treated identically for 30 min at 37°C each day before assay. $*p < 0.05$ by Student's *t* test compared with wild type. ***C***, ***D***, Expression of Fas2 (***C***, ***D***, green; ***C′***, ***D′***, white) at NMJ 4s was shown in wild type (***C***) and not affected in $NF1^{E2/E2}$ (***D***) with costained HRP in magenta. ***E***, Quantification of Fas2 levels at NMJ 4s shows no difference between wild type and $NF1^{E2/E2}$. Fas2 intensity within boutons (outlined by costained HRP) was normalized to HRP intensity quantified from the same area.

transgene restored NMJ growth in $NF1^{E2/E2}$ mutants, the A region-truncated NF1 (*CFP-NF1*Δ*A*) failed to suppress NMJ overgrowth (Fig. 4*B*). If the A region mediates a protein–protein interaction between Fak56 and NF1, overexpression of this region could disrupt the interaction and induce dominant-negative effects. Indeed, when overexpressed in presynapses, the NF1-A region significantly enhanced NMJ growth (Fig. 4*C*, bottom). As a control, overexpression of the adjacent NF1-B region (Fig. 4*A*, amino acids 400–808) had no effect on NMJ growth (Fig. 4*C*), although both proteins were expressed at equivalent levels (Fig. 4*C*, top). These results support the notion that the NF1-A region, when overexpressed, blocks the Fak56 and NF1 interaction crucial for NMJ growth regulation.

We found that the NF1 fusion protein CFP-NF1 was localized at NMJs when expressed by neuronal *elav-GAL4* (Fig. 4*D*). Interestingly, the A region-deleted NF1, CFP-NF1ΔA, failed to reveal NMJ localization (Fig. 4*E*). In addition, only CFP-NF1 signal was detected in axonal tracts. However, both proteins were expressed at similar levels as they were detected in the soma of ventral nerve cords (Fig. 4*F*, *G*). These results suggest that the A region is required for NF1 presynaptic localization.

NMJ growth regulation is independent of the GAP activity of NF1

The NF1 activity is known to modulate two signaling pathways, suppression of the Ras pathway and activation of the cAMP pathway (Shilyansky et al., 2010). We first investigated whether the RasGAP activity of NF1 that downregulates the Ras pathway contributes to NMJ growth regulation. *NF1* transgenes with mutations in the GRD were tested for their ability to rescue NMJ overgrowth in $NF1^{E2/E2}$ mutants. The arginine to proline (RP) mutation (*hs-NF1 RP*) specifically affects RasGAP activity while the lysine to alanine (KA) mutation (*hs-NF1 KA*) affects the electrostatic interaction with Ras (Walker et al., 2006). Interestingly, both transgenes, as well as the one with complete removal of GRD (*hs-NF1* Δ*GRD*), rescued the NMJ overgrowth defect in $NF1^{E2/E2}$, and their rescuing activities were comparable to wild-type *hs-NF1* (Fig. 5*A*). In contrast, transgenes with defect in GAP activity (*RP* and Δ*GRD*) did not rescue the body size of $NF1^{E2/E2}$ pupae (Fig. 5*B*), which was also reported (Walker et al., 2006). Thus, the GAP activity of NF1 is not essential in NMJ growth regulation.

To test whether NF1 regulates Ras signaling at NMJs, we examined the protein level of the cell adhesion molecule Fas2. The gene dosage of *fas2* modulates the NMJ size and the Fas2 protein level at NMJs is a sensitive readout of Ras signaling (Koh et al., 2002). We found that the Fas2 levels were indistinguishable between $NF1^{E2/E2}$ and wild-type control (Fig. 5*C*–*E*). Together, these results suggest that NF1 functions independently of the Ras pathway in regulating NMJ growth.

NMJ overgrowth in *NF1* and *Fak56* mutants is suppressed by elevating cAMP levels

NF1 functions as a regulator of ACs to modulate cellular cAMP levels (Guo et al., 1997, 2000). To test the involvement of cAMP in NF1-regulated NMJ growth, larvae were fed with food supplemented with db-cAMP or the AC activator forskolin (Tong et al., 2007). We found that the NMJ size in wild-type larvae remained the same when fed with either chemical (Fig. 6*A*). However, NMJ overgrowth in $NF1^{E2/E2}$ mutants was suppressed in both feeding conditions, compared with mock controls (Fig. 6*A*). Thus, cAMP is likely insufficient to suppress NMJ growth in *NF1* mutants.

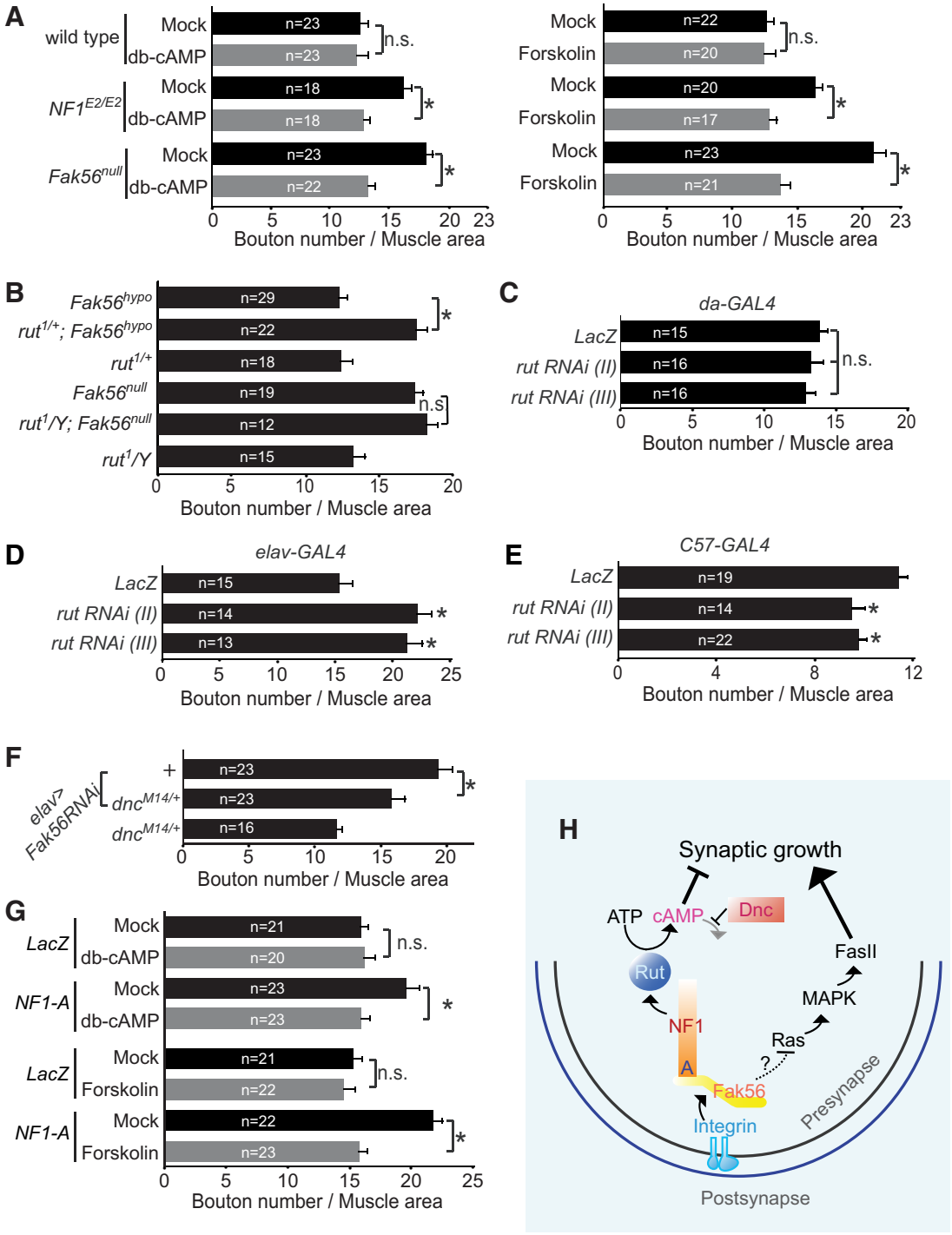

Figure 6. The cAMP pathway downstream of Fak56/NF1 in NMJ growth suppression. Quantification of NMJ 6/7 size was done as for Figure 1*C*. ***A***, Higher cAMP levels suppress NMJ overgrowth in *Fak56*^{null} and *NF1*$^{E2/E2}$. Larvae were reared in food supplemented with 10 mM db-cAMP (left) or 10 mM forskolin (right) and mock controls (black bars) are water for db-cAMP and DMSO for forskolin. *$p < 0.05$ by Student's *t* test. ***B***, *rut* enhances *Fak56*^{hypo} NMJ growth phenotype by comparing NMJ 6/7 size of *Fak56*^{hypo}, *rut*$^{1/+}$;*Fak56*^{hypo}, *rut*$^{1/+}$, *Fak56*^{null}, *rut*^{1}/Y;*Fak56*^{null}, and *rut*^{1}/Y. ***C–E***, Quantification of NMJ sizes in the depletion of *rut* by two RNAi lines (II, III) driven by *da-GAL4* (***C***), *elav-GAL4* (***D***), and *C57-GAL4* (***E***). Significant difference (*$p < 0.05$ by Student's *t* test) was compared with LacZ control. ***F***, *dnc* suppresses NMJ phenotype in neuronal expression of *Fak56RNAi* (*elav>Fak56RNAi*) by comparing with or without carrying the *dnc*^{M14} allele (*elav>Fak56RNAi; dnc*$^{M14/+}$). ***G***, Suppression of NMJ 6/7 overgrowth in neuronal expression of the A region (*elav>NF1-A*) by 10 mM db-cAMP (top) or 10 mM forskolin (bottom) compared with respective mock controls (as done for Fig. 6*A*). ***H***, Schematic drawing of presynaptic integrin signaling mediated by the AC/cAMP and Ras/MAPK pathways. See Discussion for details.

Similar to *NF1*$^{E2/E2}$, feeding *Fak56*^{null} larvae with db-cAMP or forskolin significantly suppressed NMJ overgrowth compared with the respective mock control (Fig. 6*A*). To genetically link the cAMP pathway to Fak56 signaling in NMJ growth control, *rutabaga* (*rut*) encoding the cAMP-synthesizing AC was tested for genetic interaction with *Fak56*. We found that the NMJ size in hypomorphic *Fak56*^{hypo} was enhanced by the *rut*^{1}-null allele (Fig. 6*B*), suggesting that *rut* is also involved in suppressing NMJ growth. In addition, the *rut*^{1};*Fak56*^{null} double mutant displayed the same NMJ size as the *Fak56*^{null} single mutant, consistent with

the idea that they function in the same pathway. Although the *rut*^{1} mutant shows normal NMJ growth, this might be explained by different requirements in presynaptic and postsynaptic compartments (Zhong and Wu, 1991; Zhong et al., 1992; Cheung et al., 1999). To test this, we used two independent *rut-RNAi* lines to deplete *rut* expression(Pan et al., 2009). Consistent with *rut* mutant phenotypes, depleting *rut* expression ubiquitously by *da-GAL4* showed no alteration of NMJ size (Fig. 6*C*). However, depleting *rut* expression in presynaptic neurons by *elav-GAL4* induced NMJ overgrowth, and depleting *rut* expression in muscles caused NMJ size reduction (Fig. 6*D*,*E*). We also tested the role of *dnc* encoding the cAMP-hydrolyzing phosphodiesterase in NMJ growth regulation. The NMJ overgrowth induced by presynaptic *Fak56-RNAi* knockdown (Tsai et al., 2008) was suppressed by the null *dnc*^{M14} allele (Fig. 6*F*). In summary, Fak56 functions in presynapses to maintain higher levels of cAMP, which is necessary to suppress NMJ growth.

Finally, we tested whether the interaction between Fak56 and NF1 is required in maintaining higher cAMP levels to suppress NMJ growth. The NMJ overgrowth caused by NF1-A overexpression was suppressed by the addition of either db-cAMP or forskolin to larval food (Fig. 6*G*), similar to the suppression effect on *Fak56* and *NF1* mutants. Thus, the dominant-negative effect of NF1-A, presumably disrupting the interaction between Fak56 and NF1, could be suppressed by elevating the cAMP levels during NMJ growth regulation.

Discussion

We studied *NF1* mutant phenotypes at *Drosophila* larval NMJs and found that both *Fak56* and *NF1* showed very similar phenotypes. We suggest that NF1 mediates Fak56 signaling activity through a protein–protein interaction with Fak56. The interaction with Fak56 is mediated through the N-terminal 400 aa region of NF1 that is important for NF1 function and localization. The NF1 activity in NMJ growth regulation is independent of its GAP activity but mediated through the cAMP pathway. Together with our other results (Tsai et al., 2008, 2012), these findings indicate that presynaptic Fak56 mediates integrin signaling to transduce through the NF1/AC/cAMP pathway (Fig. 6*H*). Our study reveals the role of NF1 in synapse growth modulation and its relationship with integrin/FAK signaling, which might contribute to the understanding of pathogenesis in the NF1 genetic disorder.

Integrins promote maturation of central hippocampal synapses and peripheral NMJs, mainly through the postsynaptic activity of integrin signaling (Chavis and Westbrook, 2001; Beumer et al., 2002; Schwander et al., 2004; Cingolani and Goda, 2008). The nonconventional integrin/FAK/NF1 signaling pathway identified in this study functions in the presynaptic compartment, as shown by neuronal but not muscular expression of $\beta\nu$ (Tsai et al., 2012), *Fak56* (Tsai et al., 2008), and *NF1* (Fig. 1*I*) in rescuing NMJ growth phenotypes in respective mutants. In addition to NMJ overgrowth, presynaptic release probabilities at *Fak56* and *NF1* mutant NMJs were increased, displaying enlarged EJPs and quantal contents, likely reflecting their enlarged NMJ sizes. The link between Fak56 and NF1 is mediated through the N-terminal A region of NF1 of ~400 aa. Overexpression of the A region mimicked *NF1* and *Fak56* loss-of-function mutants in inducing NMJ overgrowth suppressed by cAMP elevation. In addition, the A region is important for NF1 function in NMJ growth regulation and for NF1 localization at NMJs (Fig. 4). Previous studies define several functional domains of NF1, including the Ras GRD (Xu et al., 1990), the Leucine-rich domain (Wang et al., 2011), and the C-terminal domain (Patrakitkomjorn et al., 2008), in recruiting interacting partners, such as Ras (Xu et al., 1990), AC, syndecans (Lin et al., 2007), valosin-containing protein (Wang et al., 2011), and collapsin response mediator protein 2/4 (Lin and Hsueh, 2008). The identification of the A region in the interaction with Fak56 extends our understanding to the complex nature of NF1 regulation and activity.

Modulations of two signaling activities by NF1, the cAMP pathway and the Ras pathway, have been well studied. We showed that the GAP activity of NF1 that causes the downregulation of Ras signaling is not needed in NMJ growth regulation. Instead, the GAP activity participates in body size control and circadian rhythm in *Drosophila* (Williams et al., 2001; Walker et al., 2006). On the other hand, the cAMP regulation of NF1 is important in learning and memory (Guo et al., 2000) and life-span control (Tong et al., 2007), in addition to NMJ growth regulation. Together, our genetic analysis and feeding of cAMP analogs suggest that Fak56/NF1 signaling maintains sufficient cAMP activity in suppressing NMJ growth. The cAMP activity through activation of PKA regulates local reorganization of actin cytoskeleton (Lin et al., 2007). It could also function through the transcription factor CREB to regulate gene expression (Davis et al., 1996; Yukawa et al., 1999). Our results suggest that a threshold of cAMP levels is maintained by the Fak56/NF1 in presynapses to confine NMJ growth. The different requirements of the cAMP pathway in presynapses and postsynapses in regulating NMJ size may indicate that presynaptic and postsynaptic interaction leads to the normal size of NMJs in ubiquitous knockdown (Fig. 6*C–E*).

Fak56-mediated presynaptic integrin signaling that regulates NMJ growth is mediated through both AC/cAMP activation and Ras/MAPK inhibition (Tsai et al., 2008). NF1 is known to regulate both pathways through distinct domains (Guo et al., 1997; The et al., 1997; Hannan et al., 2006). Whereas the Ras-GAP activity of NF1 is necessary to regulate pupal size (Walker et al., 2006), this activity is dispensable in regulating NMJ growth. Furthermore, NF1 does not affect MAPK activation at NMJs, as we have detected normal phospho-ERK (data not shown) and Fas2 levels at NMJs in *NF1* mutants (Fig. 5*C–E*). How does Fak56 inhibit ERK activity at NMJs? In addition to NF1, we found that the RasGAP protein vacuolar peduncle (Vap) (Botella et al., 2003) regulates NMJ growth and genetically interacts with Fak56 in NMJ growth regulation (Wang et al., 2011; data not shown). Therefore, Fak56-mediated integrin signaling may function through both NF1 and Vap to modulate AC/cAMP and Ras/MAPK pathways, respectively, leading to the regulation of NMJ growth.

Loss of neurofibromin is the cause of the common human disorder NF1. Children with NF1, in addition to a predisposition to benign and malignant tumors, also suffer from learning and behavioral disadvantages (North et al., 1994; Cichowski and Jacks, 2001). We have shown that the N-terminal A region of NF1 is required for NF1 to interact with Fak56 at synapses. At least 18 missense mutations within the 400 aa of the A region have been identified within the corresponding region of human NF1 (according to Human Gene Mutation Database), raising the possibility that disregulation of the FAK–NF1 interaction and hence presynaptic integrin activity, if conserved in humans, may contribute to NF1 pathogenesis.

References

Allanson JE, Upadhyaya M, Watson GH, Partington M, MacKenzie A, Lahey D, MacLeod H, Sarfarazi M, Broadhead W, Harper PS (1991) Watson

syndrome: is it a subtype of type 1 neurofibromatosis? J Med Genet 28: 752–756. CrossRef Medline

Arun D, Gutmann DH (2004) Recent advances in neurofibromatosis type 1. Curr Opin Neurol 17:101–105. CrossRef Medline

Beggs HE, Schahin-Reed D, Zang K, Goebbels S, Nave KA, Gorski J, Jones KR, Sretavan D, Reichardt LF (2003) FAK deficiency in cells contributing to the basal lamina results in cortical abnormalities resembling congenital muscular dystrophies. Neuron 40:501–514. CrossRef Medline

Beumer K, Matthies HJ, Bradshaw A, Broadie K (2002) Integrins regulate DLG/FAS2 via a CaM kinase II-dependent pathway to mediate synapse elaboration and stabilization during postembryonic development. Development 129:3381–3391. Medline

Botella JA, Kretzschmar D, Kiermayer C, Feldmann P, Hughes DA, Schneuwly S (2003) Deregulation of the Egfr/Ras signaling pathway induces age-related brain degeneration in the Drosophila mutant vap. Mol Biol Cell 14:241–250. CrossRef Medline

Chavis P, Westbrook G (2001) Integrins mediate functional pre- and postsynaptic maturation at a hippocampal synapse. Nature 411:317–321. CrossRef Medline

Cheung US, Shayan AJ, Boulianne GL, Atwood HL (1999) Drosophila larval neuromuscular junction's responses to reduction of cAMP in the nervous system. J Neurobiol 40:1–13. CrossRef Medline

Cichowski K, Jacks T (2001) NF1 tumor suppressor gene function: narrowing the GAP. Cell 104:593–604. CrossRef Medline

Cingolani LA, Goda Y (2008) Differential involvement of beta3 integrin in pre- and postsynaptic forms of adaptation to chronic activity deprivation. Neuron Glia Biol 4:179–187. CrossRef Medline

Costa RM, Yang T, Huynh DP, Pulst SM, Viskochil DH, Silva AJ, Brannan CI (2001) Learning deficits, but normal development and tumor predisposition, in mice lacking exon 23a of Nf1. Nat Genet 27:399–405. CrossRef Medline

Davis GW, Schuster CM, Goodman CS (1996) Genetic dissection of structural and functional components of synaptic plasticity. III. CREB is necessary for presynaptic functional plasticity. Neuron 17:669–679. CrossRef Medline

Devenport D, Brown NH (2004) Morphogenesis in the absence of integrins: mutation of both Drosophila beta subunits prevents midgut migration. Development 131:5405–5415. CrossRef Medline

Endo M, Yamashita T (2009) Inactivation of Ras by p120GAP via focal adhesion kinase dephosphorylation mediates RGMa-induced growth cone collapse. J Neurosci 29:6649–6662. CrossRef Medline

Feng Y, Ueda A, Wu CF (2004) A modified minimal hemolymph-like solution, HL3.1, for physiological recordings at the neuromuscular junctions of normal and mutant Drosophila larvae. J Neurogenet 18:377–402. CrossRef Medline

Friedman JM (1999) Epidemiology of neurofibromatosis type 1. Am J Med Genet 89:1–6. Medline

Guo HF, The I, Hannan F, Bernards A, Zhong Y (1997) Requirement of Drosophila NF1 for activation of adenylyl cyclase by PACAP38-like neuropeptides. Science 276:795–798. CrossRef Medline

Guo HF, Tong J, Hannan F, Luo L, Zhong Y (2000) A neurofibromatosis-1-regulated pathway is required for learning in Drosophila. Nature 403: 895–898. CrossRef Medline

Gutmann DH, Boguski M, Marchuk D, Wigler M, Collins FS, Ballester R (1993) Analysis of the neurofibromatosis type 1 (NF1) GAP-related domain by site-directed mutagenesis. Oncogene 8:761–769. Medline

Hannan F, Ho I, Tong JJ, Zhu Y, Nurnberg P, Zhong Y (2006) Effect of neurofibromatosis type I mutations on a novel pathway for adenylyl cyclase activation requiring neurofibromin and Ras. Hum Mol Genet 15: 1087–1098. CrossRef Medline

Koh YH, Ruiz-Canada C, Gorczyca M, Budnik V (2002) The Ras1-mitogen-activated protein kinase signal transduction pathway regulates synaptic plasticity through fasciclin II-mediated cell adhesion. J Neurosci 22: 2496–2504. Medline

Li W, Lee J, Vikis HG, Lee SH, Liu G, Aurandt J, Shen TL, Fearon ER, Guan JL, Han M, Rao Y, Hong K, Guan KL (2004) Activation of FAK and Src are receptor-proximal events required for netrin signaling. Nat Neurosci 7:1213–1221. CrossRef Medline

Lin YL, Hsueh YP (2008) Neurofibromin interacts with CRMP-2 and CRMP-4 in rat brain. Biochem Biophys Res Commun 369:747–752. CrossRef Medline

Lin YL, Lei YT, Hong CJ, Hsueh YP (2007) Syndecan-2 induces filopodia and dendritic spine formation via the neurofibromin-PKA-Ena/VASP pathway. J Cell Biol 177:829–841. CrossRef Medline

Liu G, Beggs H, Jürgensen C, Park HT, Tang H, Gorski J, Jones KR, Reichardt LF, Wu J, Rao Y (2004) Netrin requires focal adhesion kinase and Src family kinases for axon outgrowth and attraction. Nat Neurosci 7:1222–1232. CrossRef Medline

McLachlan EM, Martin AR (1981) Non-linear summation of end-plate potentials in the frog and mouse. J Physiol 311:307–324. Medline

Mitra SK, Hanson DA, Schlaepfer DD (2005) Focal adhesion kinase: in command and control of cell motility. Nat Rev Mol Cell Biol 6:56–68. CrossRef Medline

Myers JP, Gomez TM (2011) Focal adhesion kinase promotes integrin adhesion dynamics necessary for chemotropic turning of nerve growth cones. J Neurosci 31:13585–13595. CrossRef Medline

North K, Joy P, Yuille D, Cocks N, Mobbs E, Hutchins P, McHugh K, de Silva M (1994) Specific learning disability in children with neurofibromatosis type 1: significance of MRI abnormalities. Neurology 44:878–883. CrossRef Medline

Palmer RH, Fessler LI, Edeen PT, Madigan SJ, McKeown M, Hunter T (1999) DFak56 is a novel Drosophila melanogaster focal adhesion kinase. J Biol Chem 274:35621–35629. CrossRef Medline

Pan Y, Zhou Y, Guo C, Gong H, Gong Z, Liu L (2009) Differential roles of the fan-shaped body and the ellipsoid body in Drosophila visual pattern memory. Learn Mem 16:289–295. CrossRef Medline

Patrakitkomjorn S, Kobayashi D, Morikawa T, Wilson MM, Tsubota N, Irie A, Ozawa T, Aoki M, Arimura N, Kaibuchi K, Saya H, Araki N (2008) Neurofibromatosis type 1 (NF1) tumor suppressor, neurofibromin, regulates the neuronal differentiation of PC12 cells via its associating protein, CRMP-2. J Biol Chem 283:9399–9413. CrossRef Medline

Ren XR, Ming GL, Xie Y, Hong Y, Sun DM, Zhao ZQ, Feng Z, Wang Q, Shim S, Chen ZF, Song HJ, Mei L, Xiong WC (2004) Focal adhesion kinase in netrin-1 signaling. Nat Neurosci 7:1204–1212. CrossRef Medline

Rico B, Beggs HE, Schahin-Reed D, Kimes N, Schmidt A, Reichardt LF (2004) Control of axonal branching and synapse formation by focal adhesion kinase. Nat Neurosci 7:1059–1069. CrossRef Medline

Robles E, Gomez TM (2006) Focal adhesion kinase signaling at sites of integrin-mediated adhesion controls axon pathfinding. Nat Neurosci 9:1274–1283. CrossRef Medline

Schwander M, Shirasaki R, Pfaff SL, Müller U (2004) Beta1 integrins in muscle, but not in motor neurons, are required for skeletal muscle innervation. J Neurosci 24:8181–8191. CrossRef Medline

Shi Y, Pontrello CG, DeFea KA, Reichardt LF, Ethell IM (2009) Focal adhesion kinase acts downstream of EphB receptors to maintain mature dendritic spines by regulating cofilin activity. J Neurosci 29:8129–8142. CrossRef Medline

Shilyansky C, Lee YS, Silva AJ (2010) Molecular and cellular mechanisms of learning disabilities: a focus on NF1. Annu Rev Neurosci 33:221–243. CrossRef Medline

Stevens CF (1976) A comment on Martin's relation. Biophys J 16:891–895. CrossRef Medline

The I, Hannigan GE, Cowley GS, Reginald S, Zhong Y, Gusella JF, Hariharan IK, Bernards A (1997) Rescue of a Drosophila NF1 mutant phenotype by protein kinase A. Science 276:791–794. CrossRef Medline

Tong JJ, Schriner SE, McCleary D, Day BJ, Wallace DC (2007) Life extension through neurofibromin mitochondrial regulation and antioxidant therapy for neurofibromatosis-1 in Drosophila melanogaster. Nat Genet 39:476–485. CrossRef Medline

Tong J, Hannan F, Zhu Y, Bernards A, Zhong Y (2002) Neurofibromin regulates G protein-stimulated adenylyl cyclase activity. Nat Neurosci 5:95–96. CrossRef Medline

Tsai PI, Kao HH, Grabbe C, Lee YT, Ghose A, Lai TT, Peng KP, Van Vactor D, Palmer RH, Chen RH, Yeh SR, Chien CT (2008) Fak56 functions downstream of integrin alphaPS3betanu and suppresses MAPK activation in neuromuscular junction growth. Neural Dev 3:26. CrossRef Medline

Tsai PI, Wang MY, Kao HH, Cheng YJ, Lin YJ, Chen RH, Chien CT (2012) Activity-dependent retrograde laminin A signaling regulates synapse growth at *Drosophila* neuromuscular junctions. Proc Natl Acad Sci U S A 109:17699–17704. CrossRef Medline

Ueda A, Grabbe C, Lee J, Lee J, Palmer RH, Wu CF (2008) Mutation of Drosophila focal adhesion kinase induces bang-sensitive behavior and disrupts glial function, axonal conduction and synaptic transmission. Eur J Neurosci 27:2860–2870. CrossRef Medline

von Deimling A, Krone W, Menon AG (1995) Neurofibromatosis type 1: pathology, clinical features and molecular genetics. Brain Pathol 5:153–162. CrossRef Medline

Walker JA, Tchoudakova AV, McKenney PT, Brill S, Wu D, Cowley GS, Hariharan IK, Bernards A (2006) Reduced growth of Drosophila neurofibromatosis 1 mutants reflects a non-cell-autonomous requirement for GTPase-Activating Protein activity in larval neurons. Genes Dev 20:3311–3323. CrossRef Medline

Wallace MR, Marchuk DA, Andersen LB, Letcher R, Odeh HM, Saulino AM, Fountain JW, Brereton A, Nicholson J, Mitchell AL (1990) Type 1 neurofibromatosis gene: identification of a large transcript disrupted in three NF1 patients. Science 249:181–186. CrossRef Medline

Wang HF, Shih YT, Chen CY, Chao HW, Lee MJ, Hsueh YP (2011) Valosin-containing protein and neurofibromin interact to regulate dendritic spine density. J Clin Invest 121:4820–4837. CrossRef Medline

Weiss B, Bollag G, Shannon K (1999) Hyperactive Ras as a therapeutic target in neurofibromatosis type 1. Am J Med Genet 89:14–22. Medline

Williams JA, Su HS, Bernards A, Field J, Sehgal A (2001) A circadian output in Drosophila mediated by neurofibromatosis-1 and Ras/MAPK. Science 293:2251–2256. CrossRef Medline

Woo S, Rowan DJ, Gomez TM (2009) Retinotopic mapping requires focal adhesion kinase-mediated regulation of growth cone adhesion. J Neurosci 29:13981–13991. CrossRef Medline

Xu GF, O'Connell P, Viskochil D, Cawthon R, Robertson M, Culver M, Dunn D, Stevens J, Gesteland R, White R (1990) The neurofibromatosis type 1 gene encodes a protein related to GAP. Cell 62:599–608. CrossRef Medline

Yukawa K, Tanaka T, Tsuji S, Akira S (1999) Regulation of transcription factor C/ATF by the cAMP signal activation in hippocampal neurons, and molecular interaction of C/ATF with signal integrator CBP/p300. Brain Res Mol Brain Res 69:124–134. Medline

Zhong Y, Wu CF (1991) Altered synaptic plasticity in Drosophila memory mutants with a defective cyclic AMP cascade. Science 251:198–201. CrossRef Medline

Zhong Y, Budnik V, Wu CF (1992) Synaptic plasticity in *Drosophila* memory and hyperexcitable mutants: role of cAMP cascade. J Neurosci 12:644–651. Medline